HAL
open science

Impact of the charge transfer process on the Fe2+/Fe3+distribution at Fe3O4 magnetic surface induced by deposited Pd clusters

B.S. Youmbi, C.-H. Pélisson, Audrey Denicourt-Nowicki, Alain Roucoux, Jean-Marc Greneche

To cite this version:

B.S. Youmbi, C.-H. Pélisson, Audrey Denicourt-Nowicki, Alain Roucoux, Jean-Marc Greneche. Impact of the charge transfer process on the Fe2+/Fe3+distribution at Fe3O4 magnetic surface induced by deposited Pd clusters. Surface Science : A Journal Devoted to the Physics and Chemistry of Interfaces, 2021, 712, pp.121879. 10.1016/j.susc.2021.121879 . hal-03268849

HAL Id: hal-03268849

https://hal.science/hal-03268849

Submitted on 1 Jul 2021

HAL is a multi-disciplinary open access archive for the deposit and dissemination of scientific research documents, whether they are published or not. The documents may come from teaching and research institutions in France or abroad, or from public or private research centers.

L'archive ouverte pluridisciplinaire **HAL**, est destinée au dépôt et à la diffusion de documents scientifiques de niveau recherche, publiés ou non, émanant des établissements d'enseignement et de recherche français ou étrangers, des laboratoires publics ou privés.

Impact of the charge transfer process on the Fe^{2+}/Fe^{3+} distribution at Fe_3O_4 magnetic surface induced by deposited Pd clusters

Bertrand Sitamtze Youmbi,[a,b,*] Carl-Hugo Pélisson,[c] Audrey Denicourt-Nowicki,[c] Alain Roucoux[c] and Jean-Marc Greneche[a]

[a]*IMMM UMR CNRS 6283, Institut des Molécules et Matériaux du Mans, Université du Maine, 72085 Le Mans Cedex 9, France*

[b]*Faculty of Engineering and Technology, University of Buea, P.O. Box 63, Buea, South West Region, Cameroon*

[c] *Université de Rennes, Ecole Nationale Supérieure de Chimie de Rennes, CNRS ISCR-UMR 6226, F-35000 Rennes, France*

Abstract

Magnetic iron oxide particles decorated with transition-metal nanoparticles have become increasingly attractive in catalysis regarding the environment modifications, such as an additive ligand or carrier, which could significantly influence their performances. In this work, we used the Density Functional Theory (DFT) in the gradient approximation to study the interaction between the metal and its support for palladium and palladium oxide clusters on the surface of Fe_3O_4(001)magnetite. We report a dynamic process promoted by the palladium deposition with charge transfer from the metal host. An increase in the Fe^{2+}/Fe^{3+} ratio at the topmost surface of the support was determined. The reduction of surface Fe^{3+} ions with electrons located at the interface has been proposed. Surprisingly, this slight increase in the surface density in Fe^{2+} ions was not observed in palladium oxide when the charge transfer from the support was significantly enhanced. Finally, the impact of the charge transfer process between the surface and the adsorbed species on palladium in terms of structure stability was discussed.

Keywords: Catalysis, Density Functional Theory, Palladium, Magnetite support, Charge transfer

*Corresponding author.
E-mail address: bertrand.sitamtze@ubuea.cm (B. Sitamtze Youmbi).

Journal Pre-proof

Journal Pre-proof

Highlights

- Density Functional Theory (DFT) is used to study the interaction between the metal and its support
- Palladium and palladium oxide deposition on Fe_3O_4(001) is accompanied with charge transfer from the metal host
- The charge transfer induces an increase in the Fe^{2+}/Fe^{3+} ratio at the topmost surface of the support
- The charge transfer may be more efficient for palladium oxide but the resulting structure is thermodynamically unstable

Journal Pre-proof

1. Introduction

Numerous important industrial reactions are traditionally carried out using heterogeneous noble metal-based catalysts under severe temperature and/or pressure conditions [1]. In recent decades, industry has become concerned due to economic and environmental aspects with the use of new catalysts based on Earth-abundant, low cost row transition metals, and reaction media limiting volatile organic solvents (COVs) [2, 3]. In the context of more eco-responsible chemical processes [4], the search of highly active, selective materials remains an exciting research area. Additionally, the catalyst recovery is a crucial parameter for their applicability on an industrial scale [5], as metal contamination is highly regulated, particularly in the pharmaceutical industry. Among the various strategies to separate reaction products from the catalytic media such as supported materials [6] or biphasic liquid-liquid approach [7], magnetically retrievable iron particles have appeared as appealing and sustainable supports for the immobilization of active species [8, 9, 10]. Finally, the combination of metal nanoparticles with heterogeneous magnetic support provides a powerful tool for developing new, highly active, and recyclable catalysts for relevant applications in catalysis [11].

Palladium on magnetite nanoparticles has been used as catalyst for a variety of applications such as in wastewater treatment processes through the hydrodehalogenation reactions [12] or for the hydrogenation of acetylenic to olefinic compounds [13]. Aggregated palladium atoms on magnetite have been reported as a catalyst for the Buchwald-Hartwig reaction for arylation of amines and amides [14]. The catalyst could be reused without loss in catalytic activity and reaction yield. Impregnated palladium on magnetite is one of the most used catalysts for direct arylation of heterocycles [15] and Suzuki-Miyaura cross-coupling reaction with excellent yields [16]. For many years, there was a controversy on whether single Pd atoms on iron oxide could exhibit satisfactory catalytic activity. Some authors have even reported on their inability to do so in hydrogenation of alkenes, while small Pd clusters do [17]. The introduction of Single-Atoms Catalysts (SACs) was considered as a real breakthrough due to their outstanding performance in selected industrial reactions [18, 19], though their experimental preparation is challenging. Such catalysts are useful for reactions that require high selectivity. The efficiency of Pd atoms on Fe_3O_4(001) SAC was proved for the oxidation of methanol [20]. Also, in another study by Doudin *et al.* [21], single Pd atoms on Fe_3O_4(001) structures showed effective catalytic activity on the hydrogen adsorption, dissociation and spillover. In a recent study based on density functional theory calculations, a selective hydrogenation of acetylene over single Pt, Ru, Rh, Pd, and Ir atoms supported on the Fe_3O_4(001) surface was reported, showing that the activity of the above-mentioned metals is a function of the H coverage [22]. Among the reactions for which metal supported catalysts are efficient, the oxidation of CO is one of the most studied. Chen *et al.* [23] reported a seed-mediated synthesis and evaluation of Pd/Fe_3O_4 hybrid nanoparticles with controllable interface for CO oxidation. A Pd/Fe_2O_3 nano-catalysts were synthesized by coprecipitation method, showing a great performance at low temperature [24]. Such a low temperature application of metal-magnetite catalysts was reported by Martinez-Navarro *et al.* [25] showing the efficiency of (Ag)Pd-Fe_3O_4 nanocomposites for methane oxidation. Another process for the synthesis of magnetite-supported palladium catalysts through electrospinning was reported by Malara *et al.* [26], leading to catalysts of nanofibers forms. A novel and simple microwave assisted synthesis of Pd/Fe_3O_4 nanoparticles catalyst was reported by Elazab and El-Idreesy [27], the as-prepared catalysts being potential candidates for CO oxidation and other pharmaceutical reactions. Jakub *et al.* [28] showed that the mechanism of the CO oxidation depends on whether O_2 or CO is exposed first-and therefore adsorbed- to Rh/Fe_3O_4(001) SAC.

During the last decade, several strategies for loading metal transition nanoparticles have been reported based on their immobilization on the magnetic surface, which was modified by external organic reagents [9, 29-32]. Recently,

our group reported on the preparation of nanocomposite materials such as Pd^0 or Rh^0@γ-Fe_2O_3 obtained by the deposit of the corresponding zero-valent metal nanoparticles on the non-functionalized magnetic support through a suitable wet impregnation method [33, 34]. These highly recoverable nanocomposites were characterized by TEM, XRD, ^{57}Fe Mössbauer spectrometry, X-ray photoelectron spectroscopy (XPS), and superconducting quantum interference device measurements. They were subsequently compared in the hydrogenation of various unsaturated compounds as well as in hydrodehalogenation.

In the deposition of metallic nanoparticles, the modification of the magnetic surface is known to induce electronic modification. Classically, the organic or inorganic surface coating has been developed. When considering the inorganic scheme, the interaction between a metal catalyst and its transition metal support can enhance the catalyst activity and, consequently, a higher reaction rate. In a study by Sanchez *et al.* [35], the unique catalytic capability of the dispersed Au_n(n≤20) gold cluster supported by MgO(100) was revealed, for the combustion of CO. A partial charge transfer from the surface to the cluster is shown to play a great role, with Au_8 being the smallest size to catalyze the reaction. Similarly, for the case of Pd/Mg(001) catalyst surface, Giordano *et al.*[36] reported that a strong charge transfer occurs from the substrate to adsorbed metal atoms. This charge transfer is usually associated with the donation back-donation mechanism. This charge transfer is enhanced by oxygen vacancies, with the transferred charges localized on atoms on top of the vacancies. Ahmed et *al.* [37] reported a charge transfer mechanism between platinum and MgO(100) surface, improving the water-gas shift reaction rate, an essential reaction in the fuel cell and automobile industries. Nevertheless, there are few reports on the interaction mechanism at the interface of the nanospecies and the support.

This paper reports the charge transfer process between the palladium metal extended to palladium oxide clusters and a Fe_3O_4 surface support. Based on some general considerations on the Fe_3O_4 (001) surface and computational methodology, a non-innocent charge transfer process was demonstrated at the interface.

2. Materials and Methods

2.1. General considerations

Bulk magnetite crystallizes in the inverse spinel structure of the space group Fd3m, settings 2, with oxygen ions providing a perfect face-centered cubic lattice. The Fe^{3+} ions populate the tetrahedral sites (A sites). The octahedral sites (B sites) contain both and randomly distributed Fe^{2+} and Fe^{3+} ions [38]. The stability of the different magnetite surfaces between the (111), (110) and (001) ones has been debated for several years [39-41]. Fe_3O_4(001) is a polar surface and, therefore, more catalytically favorable. There are two possible terminations for Fe_3O_4 (001) surface, which is quite dependent on the synthesis method [39]. The A-termination contains the tetrahedral iron ions. The B-termination is composed of oxygen and octahedral iron ions. Such A-termination is not so frequent but was reported to be a metastable surface [40]. The $(\sqrt{2} \times \sqrt{2})\, R45^\circ$ arrangement for Fe_3O_4 (001) surface is now well established. Unstable surfaces are generally due to surface charges, which may be reduced by reconstruction or addition of hydroxyl groups. A new approach by Pentcheva *et al.*[41] suggests that a Jahn-Teller distortion could stabilize the Fe_3O_4(001) surface. That led to a polar termination with octahedral iron and oxygen ions as the lowest energy configuration for any oxygen pressure value: this is called a modified B-terminated surface. For many years, this Distorted Bulk Truncation (DBT) structure of Fe_3O_4(001) surface was considered as stable, but failed to reproduce experimental findings on the adsorption of some metal atoms. Bliem *et al.*[42] later showed that the stable configuration is obtained by an ordered array of cation vacancies in the B-terminated surface. The obtained structure is named Subsurface Cation Vacancy (SCV) structure. This corresponds to a net removal of one cation in the previously proposed unit cell. However, the $(\sqrt{2} \times \sqrt{2})\, R45^\circ$ periodicity is maintained

by replacing two Fe_{oct} from the third layer by an interstitial Fe_{int} with tetrahedral coordination in the second layer. Therefore, the $(\sqrt{2} \times \sqrt{2})\, R45^{\circ}$ structure was considered a starting point in this work. Furthermore, since the stabilization is driven by the material adopting a stoichiometry compatible with its environment, the two top-most layers of the structures were allowed to relax along with the adsorbed Pd_{13}, or $Pd_{13}O_{12}$ cluster, while keeping the bottom layers at their bulk configuration. The structural relaxation was done using the Broyden-Fletcher-Goldfarb-Shanno (BFGS) quasi-Newton algorithm. The structured was considered as relaxed when all components of all forces are smaller than 10^{-2} a.u. and the total energy changes less than 10^{-3} a.u. between two consecutive self-consistent field steps.

2.2. Computational methodology

In quantum chemistry, individual atomic charges are not observable, though the charge density is. In this paper, these charges will be considered in the context of Löwdin analysis. Thus, the values reported here are not strictly physical charges. There is a direct correspondence between both types of charges and, therefore, the same trends. Moreover, we report only differences in charges analysis in which the errors cancel out. In population analysis, charges are calculated as a sum of the projections of the plane waves valence states $|\Psi\rangle$ onto atomic orbitals $|\Phi\rangle$. In the usual Mülliken charges analysis, the charge Q_A on an atom A is calculated using Equation (1) in which $\vec{k}$ is the wave vector, $P_{\mu\nu}(\vec{k})$ and $S_{\nu\mu}(\vec{k})$ are respectively the density matrix from the projector $P(\vec{k})$ and the overlap matrix of the atomic basis :

$$Q_A = \sum_{\vec{k}} \sum_{\mu}^{on\ A} \sum_{\nu} P_{\mu\nu}(\vec{k}) S_{\nu\mu}(\vec{k}) \tag{1}$$

with $P_{\mu\nu}(\vec{k}) = \langle \Phi^{\mu}(\vec{k}) | \hat{\rho}(\vec{k}) | \Phi^{\nu}(\vec{k}) \rangle$

and $S_{\nu\mu}(\vec{k}) = \langle \Phi_{\nu}(\vec{k}) | \Phi_{\mu}(\vec{k}) \rangle$

The subscripts represent the atomic orbitals and superscripts their corresponding duals. According to the atomic basis, which is non-orthogonal in the Mülliken analysis, the main feature of the Löwdin analysis [43, 44] is the transformation of the non-orthogonal atomic orbitals into an orthogonal set through Equation (2) [45, 46]. The reader is referred to these references for more details on the Löwdin population analysis.

$$|\Phi'_{\mu}\rangle = \sum_{\lambda} S_{\lambda\mu}^{-1/2} |\Phi_{\mu}\rangle \tag{2}$$

The Löwdin charge on atom A is therefore given by Equation (3):

$$Q_A = \sum_{\vec{k}} \sum_{\mu}^{on\ A} \sum_{\nu\lambda} S_{\mu\nu}^{1/2}(\vec{k}) P_{\nu\lambda}(\vec{k}) S_{\lambda\mu}^{1/2}(\vec{k}) \tag{3}$$

A spilling parameter is introduced to measure the difference between the plane waves eigenstates and their projections onto the atomic basis. In this work, the spilling parameter was always of 10^{-2} order, which indicates a good projection of eigenstates onto atomic orbitals. The projection is performed on atomic functions that are present in the pseudopotentials (valence states). The choice of the pseudopotentials is, therefore, the key step in such calculations. The pseudopotentials should include the wavefunctions that carry the chemistry of the atoms (3D and 4S for Fe; 2P and 3S for Mg; 2S and 2P for O; 4D, 5S and 5P for Pd) as they will be used for the projection. We have chosen the Perdew-Burke-Ernzerhof (PBE) ultra-soft pseudopotentials with an energy cut-off of 40 Ry for the wave functions and 320 Ry for charge density. Unlike hybrid functionals, Generalized Gradient Approximation (GGA) PBE pseudopotentials have been widely used for transition-metal systems [37]. Such

pseudopotentials have been shown to provide a reasonable description of the density of states, adsorption energies as well as the charge transfer between adsorbed atoms and Fe_3O_4 surfaces [47, 48]. All DFT calculations including the BFGS optimization were performed with the Quantum ESPRESSO package [49]. The Brillouin zone was sampled with a 6x6x1 Monkhorst-Pack set of k-points [50]. The structures of Pd_{13} and $Pd_{13}O_{12}$ clusters were obtained according to their bulk crystallographic symmetry, that is Fm3m (SG 225) for Pd_{13} and $P4_2/mmc$ (SG 131) for $Pd_{13}O_{12}$. The Fe_3O_4 (001) surface was represented by a slab model of five B and four A layers, making 9 layers . A vacuum of 20 Å was added in the z-direction to avoid spurious interactions. For $Pd_{13}O_{12}$ cluster, it was necessary to include the spin-orbit correction during the calculations.

The objective was the total charge and not the occupations on different orbitals. Hence all calculations were carried out within the spin-polarized GGA formalism. Although time demanding spin-polarized GGA+U is vastly used for strongly correlated material like magnetite. We have checked that discarding the Hubbard correction for such calculations and saving computational time does not significantly modify the results. The mean charge transfer for Fe_3O_4(001) from GGA calculations is -0.057e, compared to -0.062e from GGA+U, both with the same distribution over different palladium atoms. It should be pointed out that calculations on clean magnetite surfaces were found accurate without the Hubbard correction, as far as the purpose is just to study the surface stability [41]. Our assumption to discard the Hubbard correction is also supported by the fact that the magnetite surface's electronic behavior differs significantly from that of the half-metallic bulk, with a tendency to close the bandgap. Pentcheva *et al.* reported that over a broad range of oxygen pressures, the stabilization of Fe_3O_4 (001) surface goes together with a semi-metal to metal transition [41]. Such transition has also been reported for bulk magnetite [51], instead under an external compression that induces strain in the (001) plane and along the [001] direction. In the equilibrium bulk structure, the distance between the octahedrally coordinated iron atoms ($Fe_{oct.}$) and the nearest neighboring oxygen atoms (O) in bulk magnetite is 2.05Å. The semi-metal to metal transition happens when under compression, this $Fe_{oct.}$-O distance falls below a critical value of 1.99 Å [51]. On the clean Fe_3O_4(001) surface, we have obtained the distance Fe_B-O between 1.93 and 1.95 Å. This result is consistent with the above mentioned works [41, 51]. Through a more rigorous treatment, Fe_3O_4(001) surface was reported to be a semiconductor with a small bandgap of about 0.3 eV thanks to a suitable reconstruction. Though this value is very low, DFT+U calculations reveal that this surface undergoes a semiconductor-half metal transition under the effect of hydrogen adsorption, thus confirming the tendency to close the gap [52, 53].

Recently, a comparative study between the GGA and GGA+U calculations revealed that it is not mandatory to include the electronic correlation when investigating the electronic properties of the Fe_3O_4(001) surface. Furthermore, for adsorption studies, both the GGA and GGA+U exhibit the same trend whatever U's value is considered in the latter case [54]. The adsorption energy was calculated according to $E_{ads} = E_{total} - (E_{surf} + E_{clust})$ in which E_{total} corresponds to the total energy of the system. E_{surf} and E_{clust} are, the total energy of the bare surface and the on-top cluster, respectively.

In this work, apart from the Fe_3O_4(001) surface, which is our primary focus, we have included calculations on the MgO(001) surface for a better understanding of the charge transfer mechanism.

3. Results and discussion

3.1. Stability of the systems under study

The structural relaxation was performed as explained in section 2. The relaxation had little effect on the initial Pd_{13}/Fe_3O_4(001) and Pd_{13}/MgO(001) structures (Figure 1a and Figure 1b), though the Pd_{13} cluster is flattened f or

Journal Pre-proof

the latter. Figure 1c and Figure 1d display the $Pd_{13}O_{12}/Fe_3O_4(001)$ interface before and after relaxation respectively. For the first two structures, the difference between the initial and the relaxed on-top clusters is not significant, whereas a strong distortion occurs for $Pd_{13}O_{12}/Fe_3O_4(001)$ with missing bonds at the interface, especially for oxygen atoms. This is an indication of an eventual stability issue. To shed more light on this aspect, the interface atoms were deeply analyzed. The surface atoms remain almost at their clean surface positions for Pd_{13} compared to the situation observed with $Pd_{13}O_{12}$. The atoms at the surface undergo a reconstruction due to the strong interaction between the cluster and the surface.

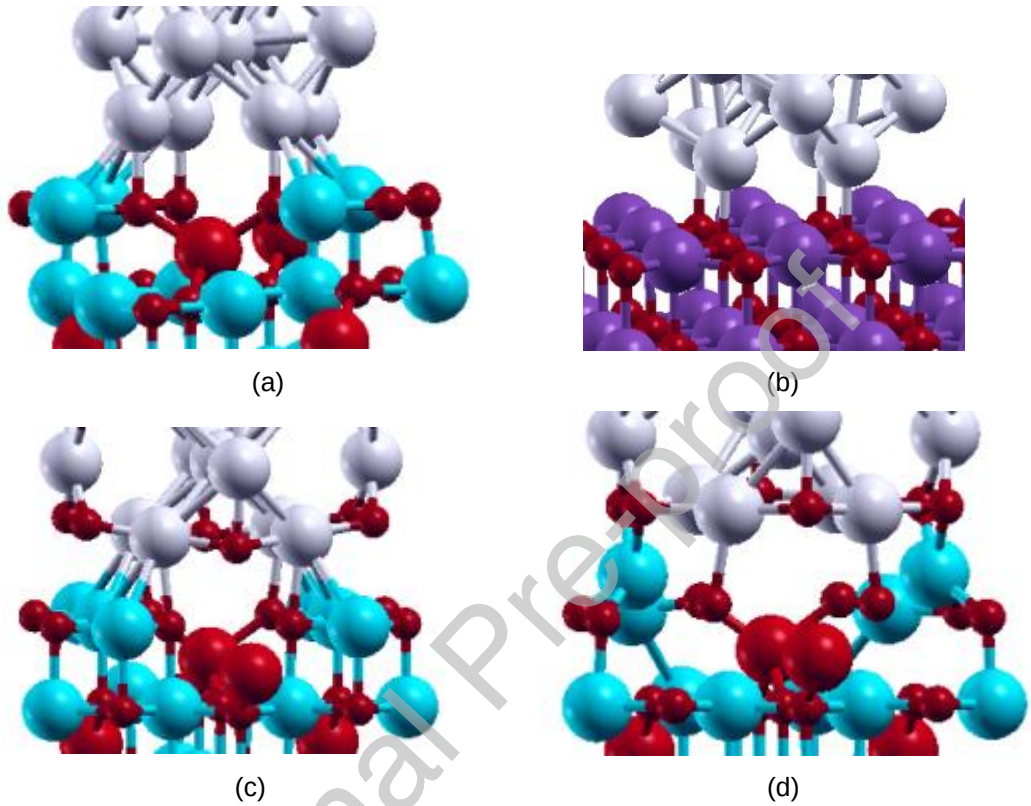

Figure 1: Structures before and after relaxation. $Pd_{13}/Fe_3O_4(001)$ (a) and $Pd_{13}/MgO(001)$ (b) show no significant effect upon relaxation. For $Pd_{13}O_{12}/Fe_3O_4(001)$ (c), the interface undergo a strong distortion (d). Color code: small red = O, large red = $Fe_{tetrahedral}$, green = $Fe_{octahedral}$, magenta = Mg, grey = Pd .

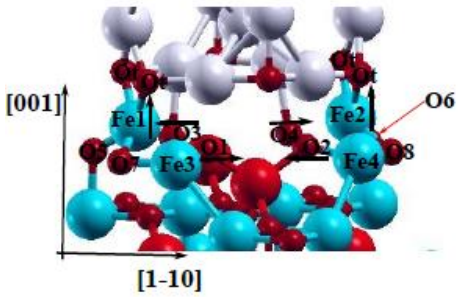

Figure 2: Details of the interface after deposition of $Pd_{13}O_{12}$ on the magnetite (001) surface. The black arrows indicate the major displacement directions for surface oxygen and iron atoms.

Figure 2 illustrates that a very strong interaction occurs at the interface if the oxygen atoms are appropriately located at the top of the surface. This is the case of Ot atoms, which interact with iron atoms at the surface,

resulting in an upwards shift of 0.85(6) Å with respect to the clean surface atomic position. The main reason for this is that these oxygen atoms tend to help the B-iron ions to recover their primary bulk octahedral coordination. In the same line, the surface oxygen atoms O3 and O4 undergo in-plane translations of -0.13(4) Å and +0.13 (4) Å along the [110] direction. The same conclusion applies to the other oxygen atoms, but instead of moving away from the [110] direction, which serves as the symmetric line for in-plane translation, O1 and O2 are moving closer together. According to Figure 3, the surface atoms could be classified in two groups and are coupled by pairs corresponding to the same in-plane and total displacement.

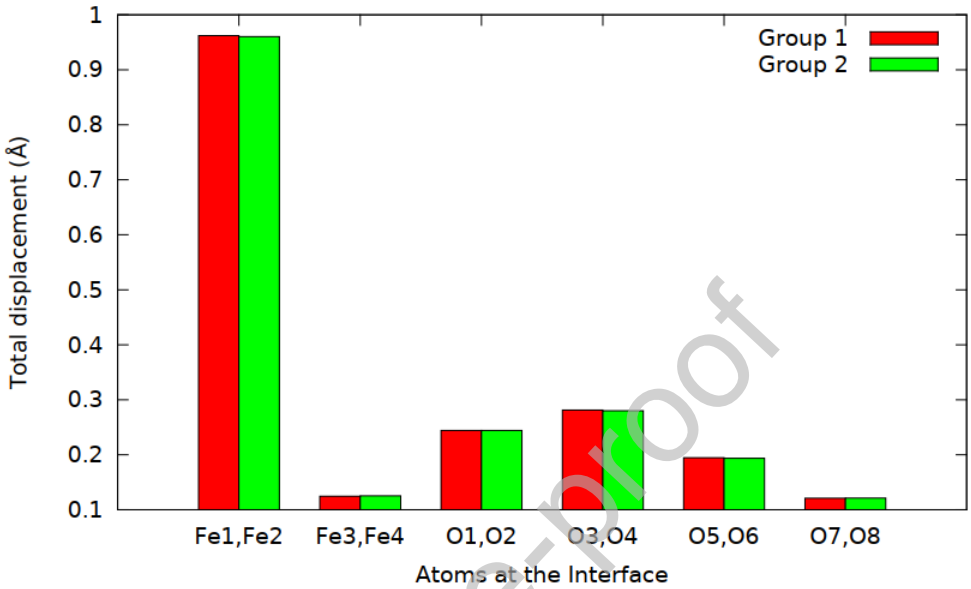

Figure 3: Total displacement for interface atoms, leading to groups of two atoms each. Distances are given with respect to their clean surface positions. See Figure 2 for atoms labelling.

From Figure 3, these two kinds of iron ions can be distinguished. The first tend to recover their bulk coordination environment, thus submitted to a strong upward shift of 0.85(6) Å, while the others correspond to iron ions, which translate smaller. Moreover, we checked the above result with Pd_{13} on the maghemite surface, which does not contain Fe^{2+} ions. We obtained similar results with respect to the reduction of the surface ions. Nevertheless, the iron vacancy at the surface induces a slightly different behavior for palladium cluster atoms. In this case, the charges that were supposed to be transferred to the missing surface iron ions remain located on the atoms of the palladium cluster. To shed light on the strange behavior of the $Pd_{13}O_{12}$ cluster, we report in Table 1 the adsorption energies for both cases.

Table 1: Adsorption energy for Pd_{13} and $Pd_{13}O_{12}$ on Fe_3O_4 (001) surface.

System	Adsorption energy (eV)
Pd_{13}/Fe_3O_4 (001)	-4.75
$Pd_{13}O_{12}/Fe_3O_4$ (001)	11.49

Journal Pre-proof

The positive adsorption energy of $Pd_{13}O_{12}$ clearly indicates that this system is not thermodynamically favorable. Hence, the adsorption of $Pd_{13}O_{12}$ on Fe_3O_4 (001) results in an unstable structure. Under realistic conditions, the treatment of the magnetite surface requires considering the oxygen atmosphere surrounding the surface. However, most DFT works related to the surface catalyst ignores the environment of the surface. If palladium is associated with oxygen (this might be similar to consider the system under a high-pressure oxygen atmosphere) before deposition on the surface as described for $Pd_{13}O_{12}$, almost all Pd atoms at the surface of the cluster were negatively charged. As the oxygen ions are also negatively charged, the cluster will disperse under electrostatic repulsion between ions. Hence, the $Pd_{13}O_{12}/Fe_3O_4$(001) structure will be discarded in the following sections.

3.2. Charge transfer mechanism

As mentioned earlier, the interaction between the metal and the support is one of the most important factors to consider when focusing on the catalytic ability of the system. In this regard, the charge transfer plays a significant role. Figure 4 displays the Pd atoms labelling in the cluster. From data listed in Table 2, it appears that the deposition of Pd_{13} on Fe_3O_4(001) surface promotes a charge transfer from the support to the metal. The charges of the neighboring atoms become more negative, as indicated in Table 3. These negative charges could be attracted either by the topmost Pd atoms since they are positively charged or by the cations on the surface of the oxide. For the MgO surface, a follow up of the time evolution of the system showed that these charges would move upwards to facilitate the charge transfer from the surface to the metal cluster [37]. After the deposition of Pd_{13} on MgO(001), the average atomic charge of the higher Pd atoms is -0.057e compared with the value reported in the literature (-0.0325e) [37]. The case of the Fe_3O_4 surface is not easy to conclude. The particularity of the Fe_3O_4(001) surface is based on the presence of Fe^{3+} ions, which are electrons deficient. Therefore, there will be a competition between the topmost Pd atoms and the Fe^{3+} of the surface.

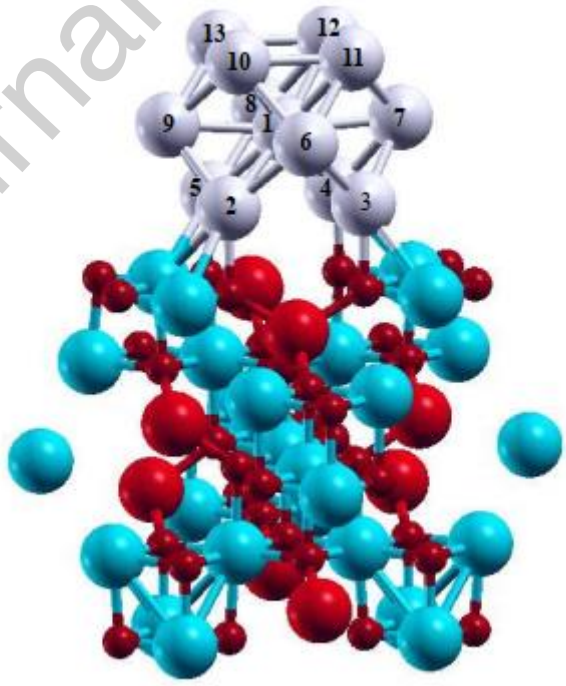

Figure 4: Labels of Pd atoms in Pd_{13} on Fe_3O_4(001). The charges on topmost Pd atoms are smaller compared to the bottom negative charges.

Table 2: Total charge differences due to the adsorption of palladium (in units of e) by Fe_3O_4(001) surface.

System	Fe_3O_4 (001)	All surface atom	Only surface Fe-ions	On-top cluster
Pd_{13}/Fe_3O_4	+0.598	+0.557	-0.103	-0.752

Moreover, the density of positively charged Pd atoms is relatively low. It is likely that the presence of more electrons at the interface will result in the reduction of surface Fe^{3+} ions, increasing the Fe^{2+}/Fe^{3+} ratio in an entire experimental sample. This result is indeed in agreement with the experimental work reported by Coker *et al.* [55]. Using X-ray Magnetic Circular Dichroism (XMCD) spectra, the Fe^{2+}/Fe^{3+} ratio increased from 0.64 (more than the stoichiometric magnetite ratio) to 0.70 after the deposition of palladium nanoparticles on the surface of the biomagnetite, indicating the reduction of Fe^{3+} ions.

Table 3: Löwdin charges differences for Pd_{13} after deposition on Fe_3O_4 and MgO surfaces. All charges were given with respect to the situation in the palladium cluster alone, in units of the elementary charge e. The central atom (index 1) always losses charges. See Figure 4 for atoms labelling.

Pd atom index	Fe_3O_4(001) with Pd_{13}	MgO(001) with Pd_{13}
1	0.0483	0.1529
2	-0.2057	-0.1711
3	-0.2057	-0.1687
4	-0.1937	-0.1694
5	-0.1937	-0.1701
6	-0.0314	-0.0645
7	-0.03	-0.0385
8	-0.0297	-0.0581
9	-0.03	-0.0435
10	0.0266	0.0126
11	0.0266	0.0077
12	0.0328	0.0081
13	0.0328	0.0142

According to the literature, a clean, stable Fe_3O_4(001) only consists of Fe^{3+} ions [56]. Partial hydrogenation introduces Fe^{2+} and upon saturation, only Fe^{2+} ions are present because all Fe^{3+} has been reduced [52]. The modifications of the surface Fe ions charges are displayed in Table 4.

Table 4: Charge modification on surface Fe ions (in units of e). See Figure 2 for atoms indexes.

Fe-ion	Fe_3O_4 (001)

Journal Pre-proof

index	with Pd_{13}
Fe1	-0.0273
Fe2	-0.0273
Fe3	-0.0242
Fe4	-0.0242

3.3. Density of states

The computed Density Of States (DOS) described in Figure 5 for a clean Fe_3O_4 (001) is in good agreement with previously reported DOS. A zero DOS is expected to appear at about 0.4 eV for the majority states of the B-terminated surface [41, 54]. This feature is present in the DOS, but around -0.9 eV. This discrepancy could be explained by the fact that our DOS does not account for the electron correlation. In addition, our calculations were performed with ultra-soft pseudopotentials whereas Pentcheva *et al.* [41] reported Full-Potential Augmented Plane Wave (FP-APW) calculations. It is also for these reasons that the minimum for the minority channel is located at -0.15 eV instead of 0.0 eV as reported by Sun *et al.* [54].

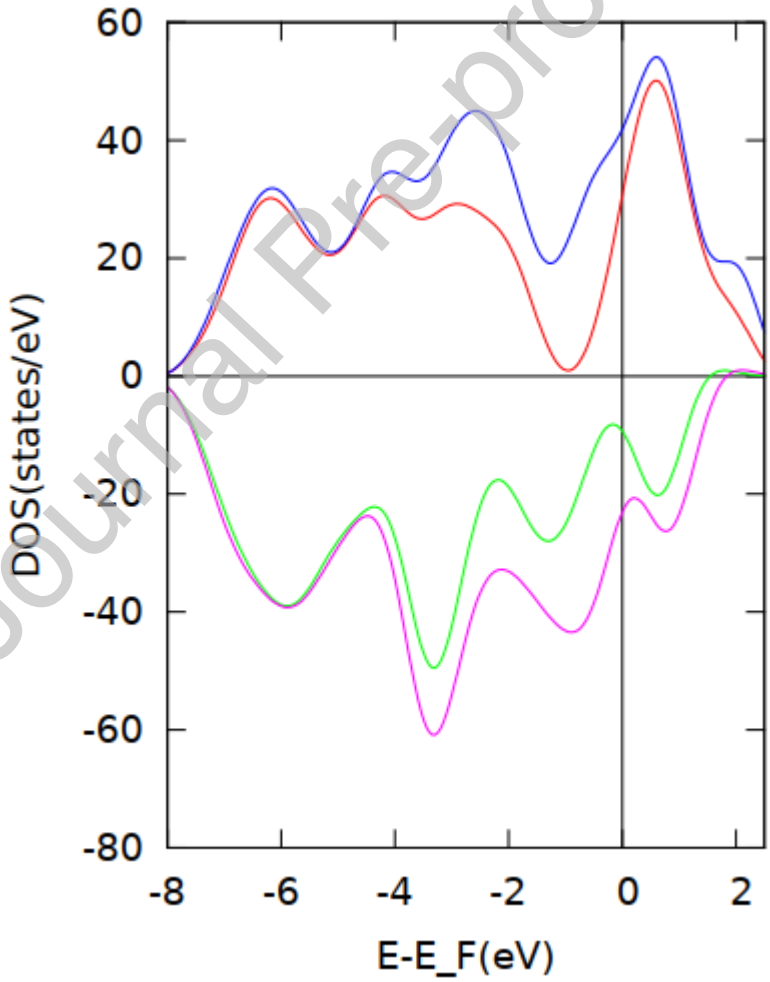

Figure 5: Total DOS of Pd_{13}/Fe_3O_4 (001). The red and green plots are respectively the spin up and spin down DOS before deposition of the on-top cluster while the blue and magenta curves represent the same DOS after adsorption.

Journal Pre-proof

Upon adsorption of Pd_{13}, a significant increase was observed in the DOS at the Fermi level[1], leading to a metallic state. We note that such a transition was already reported for Fe_3O_4(001) under hydrogen adsorption [52, 53]. It is already established that the states at the Fermi level have the t_{2g} character [57]. Therefore, an enhancement in the states at the Fermi level, as observed in Figure 5 indicates an increasing number of Fe^{2+} at the surface. This is in agreement with conclusion drawn from the Löwdin charges analysis in subsection 3.2.

4. Conclusion

The behaviour of Pd and Pd-oxide during adsorption on the iron oxide Fe_3O_4(001) surface was studied. As already described in the literature for other surfaces such as MgO(001), a charge transfer occurs between the surface and the adsorbed species, and should typically be associated with a donation-back-donation mechanism. Our calculations have shown that the adsorption of Pd increases the Fe^{2+}/Fe^{3+} ratio only at the topmost surface layer. The adsorption leads to a metallic behaviour by enhancement of the Density Of States at the Fermi Level. The charge transfer may be more efficient for palladium oxide but the resulting structure is thermodynamically unstable and may require additional treatment for practical applications. It is worth noting that in this work, other adsorption configurations different from the one considered were not investigated. Also, as the present study only deals with the system immediately after deposition on the surface, a further study involving the time evolution might be necessary, particularly for the case of palladium oxide, which is not thermodynamically favourable.

Author Statement

We the undersigned declare that this manuscript is original, has not been published before and is not currently being considered for publication elsewhere.

We confirm that the manuscript has been read and approved by all named authors and that there are no other persons who satisfied the criteria for authorship but are not listed.

We further confirm that the order of authors listed in the manuscript has been approved by all of us.

We understand that the Corresponding Author is the sole contact for the Editorial process. He responsible for communicating with the other authors about progress, submissions of revisions and fin approval of proofs.

Journal Pre-proof

[1] The modification of the DOS due to the adsorption is not substantial for states far away from the Fermi Level. But the adsorption of $Pd_{13}O_{12}$ affects considerably some deeper states around 20eV

Declaration of interests

The authors declare the following financial interests/personal relationships which may be considered as potential competing interests

Acknowledgements

This research project MAGFOCAT was supported by the Région Bretagne (C.-H. Pélisson Ph.D. fellowship). This study was also partially supported by French-Mexican ANR MINAFC-CONACyT (Mexico) grant no. 139292.

Journal Pre-proof

References

[1] Modern Heterogeneous Catalysis: An Introduction, ed R. A. van Santen, Wiley-VCH Verlag GmbH & Co. KGaA, 2017

[2] D. Wang, D. Astruc, The recent development of efficient Earth-abundant transition-metal nanocatalysts, Chem. Soc. Rev. 46 (2017) 816-854. https://doi.org/10.1039/C6CS00629A.

[3] M. Kaushik, A. Moores, New trends in sustainable nanocatalysis: Emerging use of earth abundant metals, Curr. Opin. Green Sustain. Chem. 7 (2017) 39-45. https://doi.org/10.1016/j.cogsc.2017.07.002.

[4] P. J. Dunn, The importance of Green Chemistry in Process Research and Development, Chem. Soc. Rev. 41 (2012) 1452-1461. https://doi.org/10.1039/C1CS15041C.

[5] D. J. Cole-Hamilton, R. P. Tooze, Catalyst Separation, Recovery and Recycling: Chemistry and Process Design, Springer, 2006

[6] J. M Campelo, D. Luna, R. Luque, J. M. Marinas, A. A. Romero, Sustainable Preparation of Supported Metal Nanoparticles and Their Applications in Catalysis, ChemSusChem, 2 (2009) 18-45. https://doi.org/10.1002/cssc.200800227.

[7] A. Denicourt-Nowicki, A. Roucoux, Odyssey in Polyphasic Catalysis by Metal Nanoparticles, Chem. Rec. 16 (2016) 2127-2141. https://doi.org/10.1002/tcr.201600050.

[8] L. M. Rossi, N. J. S. Costa, F. P. Silva, R. Wojcieszak, Magnetic nanomaterials in catalysis: advanced catalysts for magnetic separation and beyond, Green Chem**.** 16 (2014) 2906-2933. https://doi.org/10.1039/C4GC00164H.

[9] V. Polshettiwar, R. Luque, A. Fihri, H. Zhu, M. Bouhrara, J.-M. Basset, Magnetically Recoverable Nanocatalysts, Chem. Rev. 111 (2011) 3036-3075. https://doi.org/10.1021/cr100230z.

[10] D. Wang, D. Astruc, Fast-Growing Field of Magnetically Recyclable Nanocatalysts, Chem. Rev. 114 (2014) 6949-6985. https://doi.org/10.1021/cr500134h.

[11] S. Shylesh, W. R. Thiel, V. Schünemann, Magnetically Separable Nanocatalysts: Bridges between Homogeneous and Heterogeneous Catalysis, Angew. Chem. Int. Ed. 49 (2010) 3428-3459. https://doi.org/10.1002/anie.200905684.

[12] H. Hildebrand, K. Mackenzie, F.-D. Kopinke, Pd/Fe_3O_4 nano-catalysts for selective dehalogenation in wastewater treatment processes-Influence of water constituents, Applied Catalysis B: Environmental 91 (2009) 389-396. https://doi.org/10.1016/j.apcatb.2009.06.006.

Journal Pre-proof

[13] F. P. da Silva, L. M. Rossi, Palladium on magnetite: magnetically recoverable catalyst for selective hydrogenation of acetylenic to olefinic compounds, Tetrahedron 70 (2014) 3314-3318. https://doi.org/10.1016/j.tet.2013.10.051.

[14] S. Sá, M. B. Gawande, A. Velhinho, J. P. Veiga, N. Bundaleski, J. Trigueiro, A. Tolstogouzov, O. M. N. D. Teodoro, R. Zboril, R. S. Varma, P. S. Branco, Magnetically recyclable magnetite-palladium (Nanocat-Fe-Pd) nanocatalyst for the Buchwald–Hartwig reaction, Green Chem. 16 (2014) 3494-3500. https://doi.org/10.1039/C4GC00558A.

[15] R. Cano, J. M. Pérez, D. J. Ramón, G. P. McGlacken, Impregnated palladium on magnetite as catalyst for direct arylation of heterocycles, Tetrahedron 72 (2016) 1043-1050. https://doi.org/10.1016/j.tet.2015.12.039.

[16] R. Cano, D. J. Ramón, M. Yus, Impregnated palladium on magnetite, a new catalyst for the ligand-free cross-coupling Suzuki–Miyaura reaction, Tetrahedron 67 (2011) 5432-5436. https://doi.org/10.1016/j.tet.2011.05.072.

[17] M. D. Rossell, F. J. Caparrós, I. Angurell, G. Muller, J. Llorca, M. Secob, O. Rossell, Magnetite-supported palladium single-atoms do not catalyse the hydrogenation of alkenes but small clusters do, Catal. Sci. Technol. 6 (2016) 4081-4085. https://doi.org/10.1039/C6CY00596A.

[18] X.-F. Yang, A. Wang, B. Qiao, J. Li, J. Liu, T. Zhang, Single-Atom Catalysts: A New Frontier in Heterogeneous Catalysis, Acc. Chem. Res. 46 (2013) 1740-1748. https://doi.org/10.1021/ar300361m.

[19] G. S. Parkinson, Single-Atom Catalysis: How Structure Influences Catalytic Performance, Catalysis Letters 149 (2019) 1137-1146. https://doi.org/10.1007/s10562-019-02709-7.

[20] M. D. Marcinkowski, S. F. Yuk, N. Doudin, R. S. Smith, M.-T. Nguyen, B. D. Kay, V.-A. Glezakou, R. Rousseau, Z. Dohnálek, Low-Temperature Oxidation of Methanol to Formaldehyde on a Model Single-Atom Catalyst: Pd Atoms on Fe_3O_4(001), ACS Catal. 9 (2019) 10977-10982. https://doi.org/10.1021/acscatal.9b03891.

[21] N. Doudin, S. F. Yuk, M. D. Marcinkowski, M. -T. Nguyen, J.-C. Liu, Y. Wang, Z. Novotny, B. D. Kay, J. Li, V.-A. Glezakou, G. Parkinson, R. Rousseau, Z. Dohnálek, Understanding Heterolytic H2 Cleavage and Water-Assisted Hydrogen Spillover on Fe_3O_4(001)-Supported Single Palladium Atoms, ACS Catal. 9 (2019) 7876-7887. https://doi.org/10.1021/acscatal.9b01425.

[22] S. F. Yuk, G. Collinge, M.-T. Nguyen, M.-S. Lee, V. -A. Glezakou, R. Rousseau, Selective acetylene hydrogenation over single metal atoms supported on Fe_3O_4(001): A first-principle study, J. Chem. Phys. 152 (2020) 154703. https://doi.org/10.1063/1.5142748.

[23] S. Chen, R. Si, E. Taylor, J. Janzen, J. Chen, Synthesis of Pd/Fe_3O_4 Hybrid Nanocatalysts with Controllable Interface and Enhanced Catalytic Activities for CO Oxidation, J. Phys. Chem. C 116 (2012) 12969-12976. https://doi.org/10.1021/jp3036204.

Journal Pre-proof

[24] F. Wang, Y. Xu, K. Zhao, D. He, Preparation of Palladium Supported on Ferric Oxide Nano-catalysts for Carbon Monoxide Oxidation in Low Temperature, Nano-Micro Lett. 6 (2014) 233-241. https://doi.org/10.1007/BF03353787.

[25] B. Martinez-Navarro, R. Sanchis, E. Asedegbega-Nieto, B. Solsona, F. Ivars-Barcelo, (Ag)Pd-Fe_3O_4 Nanocomposites as Novel Catalysts for Methane Partial Oxidation at Low Temperature, Nanomaterials 10 (2020) 988. https://doi.org/10.3390/nano10050988.

[26] A. Malara, E. Paone, L. Bonaccorsi, F. Mauriello, A. Macario, P. Frontera, Pd/Fe_3O_4 Nanofibers for the Catalytic Conversion of Lignin-Derived Benzyl Phenyl Ether under Transfer Hydrogenolysis Conditions, Catalysts 10 (2020) 20. https://doi.org/10.3390/catal10010020.

[27] H. A. Elazab, T. T. El-Idreesy, Optimization of the catalytic performance of Pd/Fe_3O_4 nanoparticles prepared via microwave-assisted synthesis for pharmaceutical and catalysis applications, Biointerface Research in Applied Chemistry, 9 (2019) 3794-3799. https://doi.org/10.33263/BRIAC91.794799.

[28] Z. Jakub, J. Hulva, P. T. P. Ryan, D. A. Duncan, D. J. Payne, R. Bliem, M. Ulreich, P. Hofegger, F. Kraushofer, M. Meier, M. Schmid, U. Diebold G. S. Parkinson, Adsorbate-induced structural evolution changes the mechanism of CO oxidation on a Rh/Fe_3O_4(001) model catalyst, Nanoscale 12 (2020) 5866-5875. DOI: 10.1039/c9nr10087c.

[29] R. Hudson, Y. Feng, R. S Varma. A. Moores, Bare magnetic nanoparticles: sustainable synthesis and applications in catalytic organic transformations, Green Chem. 16 (2014) 4493-4505. https://doi.org/10.1039/C4GC00418C.

[30] R. B. Nasir Baig, R. S. Varma, Magnetic Carbon-Supported Palladium Nanoparticles: An Efficient and Sustainable Catalyst for Hydrogenation Reactions, ACS Sustainable Chem. Eng. 2 (2014) 2155-2158. https://doi.org/10.1021/sc500341h.

[31] R. B. Nasir Baig, R. S. Varma, Magnetic Silica-Supported Ruthenium Nanoparticles: An Efficient Catalyst for Transfer Hydrogenation of Carbonyl Compounds, ACS Sustainable Chem. Eng. 1 (2013) 805-809. https://doi.org/10.1021/sc400032k.

[32] R. B. Nasir Baig, R. S. Varma, A facile one-pot synthesis of ruthenium hydroxide nanoparticles on magnetic silica: aqueous hydration of nitriles to amides, Chem. Commun. 48 (2012) 6220-6222. https://doi.org/10.1039/C2CC32566G.

[33] C.-H. Pélisson, A. Denicourt-Nowicki, C. Meriadec, J.-M. Greneche, A. Roucoux, Magnetically Recoverable Palladium(0) Nanocomposite Catalyst for Hydrogenation Reactions in Water, ChemCatChem 7 (2015) 309-315. https://doi.org/10.1002/cctc.201402761.

Journal Pre-proof

[34] C.-H Pélisson, A. Denicourt-Nowicki, A. Roucoux, Magnetically Retrievable Rh(0) Nanocomposite as Relevant Catalyst for Mild Hydrogenation of Functionalized Arenes in Water, ACS Sustainable Chem. Eng. 4 (2016) 1834-1839. https://doi.org/10.1021/acssuschemeng.6b00045.

[35] A. Sanchez, S. Abbet, U. Heiz, W.-D. Schneider, H. Hakkinen, R. N. Barnett, U. Land-man, When Gold Is Not Noble: Nanoscale Gold Catalysts, J. Phys. Chem. A 103 (1999) 9573-9578. https://doi.org/10.1021/jp9935992.

[36] L. Giordano, J. Goniakowski, G. Pacchioni, Characteristics of Pd adsorption on the MgO(100) surface: Role of oxygen vacancies, Phys. Rev. B 64 (2001) 075417. https://doi.org/10.1103/PhysRevB.64.075417.

[37] F. Ahmed, R. Miura, N. Hatakeyama, H. Takaba, A. Miyamoto, D. R. Salahub, Quantum Chemical Molecular Dynamics Study of the Water-Gas Shift Reaction on a Pd/MgO(100) Catalyst Surface, J. Phys. Chem. C 117 (2013) 5051-5066. https://doi.org/10.1021/jp310946x.

[38] M. E. Fleet, The structure of magnetite, Acta Cryst. B37 (1981) 917-920. https://doi.org/10.1107/S0567740881004597.

[39] B. Stanka, W. Hebenstreit, U. Diebold, S. A. Chambers, Surface reconstruction of Fe_3O_4(001), Surf. Sc. 448 (2000) 49-63. https://doi.org/10.1016/S0039-6028(99)01182-6.

[40] G. S. Parkinson, Z. Novotny, P. Jacobson, M. Schmid, U. Diebold, A metastable Fe(A) termination at the Fe_3O_4(001) surface, Surf. Sc. 605 (2011) L42-L45. https://doi.org/10.1016/j.susc.2011.05.018.

[41] R. Pentcheva, F. Wendler, H. L. Meyerheim, W. Moritz, N. Jedrecy, M. Scheffler, Jahn-Teller Stabilization of a "Polar" Metal Oxide Surface: Fe_3O_4(001), Phys. Rev. Lett. 94 (2005) 126101. https://doi.org/10.1103/PhysRevLett.94.126101.

[42] R. Bliem, E. McDermott, P. Ferstl, M. Setvin, O. Gamba, J. Pavelec, M. A. Schneider, M. Schmid, U. Diebold, P. Blaha, L. Hammer, G. S. Parkinson, Subsurface cation vacancy stabilization of the magnetite (001) surface, Science 346 (2014) 1215-1218. DOI: 10.1126/science.1260556.

[43] P.-O. Löwdin, On the Non-Orthogonality Problem Connected with the Use of Atomic Wave Functions in the Theory of Molecules and Crystals, J. Chem. Phys. 18 (1950) 365. https://doi.org/10.1063/1.1747632.

[44] D. Sanhez-Portal, E. Artacho, J. M. Soler, Projection of plane-wave calculations into atomic orbitals, Solid State Commun. 95 (1995) 685-690. https://doi.org/10.1016/0038-1098(95)00341-X.

[45] L. C. Cusachs, P. Politzer, On the problem of defining the charge on an atom in a molecule, Chem. Phys. Lett. 1 (1968) 529-531. https://doi.org/10.1016/0009-2614(68)80010-7.

[46] P.-O. Löwdin, On the Nonorthogonality Problem, Adv. Quantum Chem. 5 (1970) 185-199. https://doi.org/10.1016/S0065-3276(08)60339-1.

Journal Pre-proof

[47] T. Pabisiak, M. J. Winiarski, T. Ossowskia, A. Kiejna, Adsorption of gold subnano-structures on a magnetite(111) surface and their interaction with CO, Phys. Chem. Chem. Phys. 18 (2016) 18169-1817 9. https://doi.org/10.1039/C6CP03222B.

[48] X. Yu, S.-G. Wang, Y.-W. Li, J. Wang, H. Jiao, Single Gold Atom Adsorption on the Fe_3O_4(111) Surface, J . Phys. Chem. C 116 (2012) 10632-10638. https://doi.org/10.1021/jp301313u .

[49] P. Giannozzi , S. Baroni, N. Bonini, M. Calandra, R. J. Car, C. Cavazzoni, D. Ceresoli, G. L Chiarotti, M. Cococcioni, I. Dabo, A. Dal Corso, S. de Gironcoli, S. Fabris, G. Fratesi, R. Gebauer, U. Gerstmann, C. Gougoussis, A. Kokalj, M. Lazzeri, L. Martin-Samos, N. Marzari, F. Mauri, R. Mazzarello, S. Paolini, A. Pasquarello, L. Paulatto, C. Sbraccia, S. Scandolo, G. Sclauzero, A. P. Seitsonen, A. Smogunov, P. Umari R. M. Wentzcovitch, QUANTUM ESPRESSO: a modular and open-source software project for quantum simulations of materials, J. Phys.: Condens. Matter 21 (2009) 395502. https://doi.org/10.1088/0953-8984/21/39/395502.

[50] H. J. Monkhorst, J. D. Pack, Special points for Brillouin-zone integrations, Phys. Rev. B 13 (1976) 5188. https://doi.org/10.1103/PhysRevB.13.5188.

[51] M. Friak, A. Schindlmayr, M. Scheffler, Ab initio study of the half-metal to metal transition in strained magnetite, New J. Phys. 9 (2007) 5. https://doi.org/10.1088/1367-2630/9/1/005.

[52] G. S. Parkinson, N. Mulakaluri, Y. Losovyj, P. Jacobson, R. Pentcheva, U. Diebold, Semiconductor-half metal transition at the Fe_3O_4(001) surface upon hydrogen adsorption, Phys. Rev. B 82 (2010) 125413. https://doi.org/10.1103/PhysRevB.82.125413.

[53] M. Kurahashi, X. Sun, Y. Yamauchi, Recovery of the half-metallicity of an Fe_3O_4(100) surface by atomic hydrogen adsorption, Phys. Rev. B 81 (2010) 193402. https://doi.org/10.1103/PhysRevB.81.193402.

[54] X. Sun, M. Kurahashi, A. Pratt, Y. Yamauchi, First-principles study of atomic hydrogen adsorption on Fe_3O_4(100), Surf. Sc. 605 (2011) 1067-1073. https://doi.org/10.1016/j.susc.2011.03.006.

[55] V. S. Coker, J. A. Bennett, N. D. Telling, T. Henkel, J. M. Charnock, G. van der Laan, R. A. D. Pattrick, C. I. Pearce, R. S. Cutting, I. J. Shannon, J. Wood, E. Arenholz, I. C. Lyon, J. R. Lloyd, Microbial Engineering of Nanoheterostructures: Biological Synthesis of a Magnetically Recoverable Palladium Nanocatalyst, ACS Nano. 4 (2010) 2577-2584. https://doi.org/10.1021/nn9017944.

[56] N. Mulakaluri, R. Pentcheva, M. Wieland, W. Moritz, M. Scheffler, Partial Dissociation of Water on Fe_3O_4(001): Adsorbate Induced Charge and Orbital Order, Phys. Rev. B 103 (2009) 176102. https://doi.org/10.1103/PhysRevLett.103.176102.

Journal Pre-proof

[57] Z. Zhang, S. Satpathy, Electron states, magnetism, and the Verwey transition in magnetite, Phys. Rev. B 44 (1991) 13319. https://doi.org/10.1103/PhysRevB.44.13319.

Journal Pre-proof

Graphical_Abstract

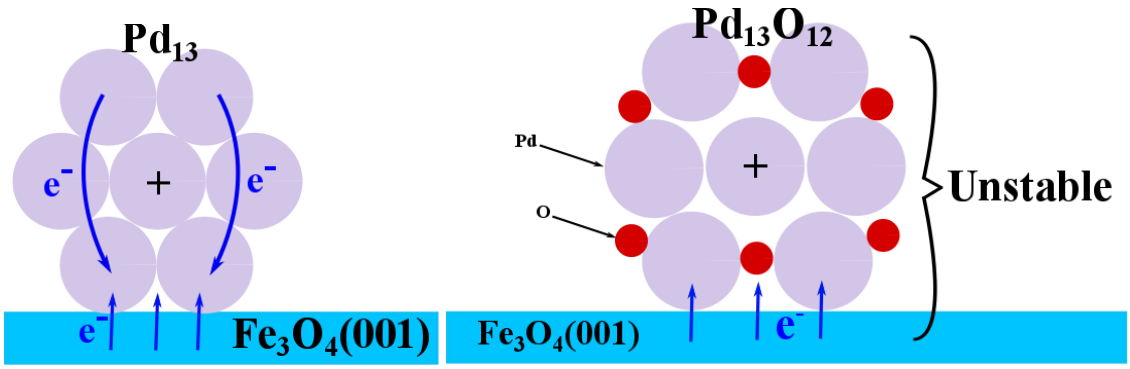

Journal Pre-proof